A heterodimer formed by bone morphogenetic protein 9 (BMP9) and BMP10 provides most BMP biological activity in plasma

Emmanuelle Tillet, Marie Ouarné, Agnès Desroches-Castan, Christine Mallet, Mariela Subileau, Robin Didier, Anna Lioutsko, Guillaume Belthier, Jean-Jacques Feige, Sabine Bailly

A heterodimer formed by bone morphogenetic protein 9 (BMP9) and BMP10 provides most BMP biological activity in plasma

Received for publication, March 17, 2018, and in revised form, May 4, 2018 Published, Papers in Press, May 22, 2018, DOI 10.1074/jbc.RA118.002968

Emmanuelle Tillet[1], **Marie Ouarné**[2], **Agnès Desroches-Castan, Christine Mallet, Mariela Subileau, Robin Didier**[3], **Anna Lioutsko**[4], **Guillaume Belthier**[5], **Jean-Jacques Feige, and Sabine Bailly**

From the University of Grenoble Alpes, Inserm, CEA, BIG-Biologie du Cancer et de l'Infection, 38000 Grenoble, France

Edited by Phyllis I. Hanson

Bone morphogenetic protein 9 (BMP9) and BMP10 are the two high-affinity ligands for the endothelial receptor activin receptor-like kinase 1 (ALK1) and are key regulators of vascular remodeling. They are both present in the blood, but their respective biological activities are still a matter of debate. The aim of the present work was to characterize their circulating forms to better understand how their activities are regulated *in vivo*. First, by cotransfecting BMP9 and BMP10, we found that both can form a disulfide-bonded heterodimer *in vitro* and that this heterodimer is functional on endothelial cells via ALK1. Next, we developed an ELISA that could specifically recognize the BMP9–BMP10 heterodimer and which indicated its presence in both human and mouse plasma. In addition to using available *Bmp9*-KO mice, we generated a conditional *Bmp10*-KO mouse strain. The plasma from *Bmp10*-KO mice, similarly to that of *Bmp9*-KO mice, completely lacked the ability to activate ALK1-transfected 3T3 cells or phospho-Smad1–5 on endothelial cells, indicating that the circulating BMP activity is mostly due to the BMP9–BMP10 heterodimeric form. This result was confirmed in human plasma that had undergone affinity chromatography to remove BMP9 homodimer. Finally, we provide evidence that hepatic stellate cells in the liver could be the source of the BMP9–BMP10 heterodimer. Together, our findings demonstrate that BMP9 and BMP10 can heterodimerize and that this heterodimer is responsible for most of the biological BMP activity found in plasma.

This work was supported in part by INSERM (Institut National de la Santé et de la Recherche Médicale, U1036), CEA (Commisariat à l'Energie Atomique et aux Energies Alternatives, DRF/BIG/BCI), UGA (University Grenoble-Alpes), the Ligues Départementales contre le Cancer de la Loire et de la Savoie, the association Maladie de Rendu-Osler (AMRO), the Fondation pour la Recherche Médicale (FRM), and the Association Pour la Recherche sur le Cancer. The authors declare that they have no conflicts of interest with the contents of this article.
This article contains Figs. S1–S7.

[1] To whom correspondence should be addressed: UMR1036 CEA-G/BIG/BCI, 17 rue des Martyrs, 38054 Grenoble Cedex, France. Tel.: 33-438784464; Fax: 33-438785058; E-mail: emmanuelle.tillet@cea.fr.
[2] Supported by the Ph.D. program of CEA/DSV (IRTELIS).
[3] Present address: University of Nice, INSERM, C3M, 06200 Nice, France.
[4] Present address: University of Paris Sud 11, INSERM, CEA, IDMIT, 92260 Fontenay-aux-Roses, France.
[5] Present address: University of Montpellier, INSERM, CNRS, IGF, 34090 Montpellier, France.

Bone morphogenetic proteins (BMPs)[6] are members of the transforming growth factor β (TGFβ) superfamily that regulate cellular events essential for embryonic development and tissue homeostasis (1).

BMPs are synthesized as pro-proteins, consisting of an N-terminal prodomain, and a receptor-binding C-terminal mature region (2). A single disulfide bond within the terminal mature region allows dimerization of the pro-protein, which is further processed through proteolytic cleavage by furin proconvertases (3, 4). BMP homodimers bind to and activate a receptor complex consisting of two type I and type II transmembrane serine/threonine kinases (5). Following ligand binding, activated receptors propagate signaling by phosphorylating the receptor-regulated SMAD1, -5, or -8, which, in association with SMAD4, translocate to the cell nucleus and regulate expression of the SMAD pathway-responsive genes (6).

Among the TGFβ growth factor family, BMP9 and BMP10 are two high-affinity ligands for the endothelial-specific type I receptor activin receptor-like kinase 1 (ALK1) and its co-receptor endoglin (7, 8). The signaling pathway activated through these receptors is critical for vascular development. Indeed, mutations in *ACVLR1*, encoding ALK1, or *ENG*, encoding endoglin, cause an autosomal dominant disease, hereditary hemorrhagic telangiectasia (HHT), characterized by vascular disorders including abundant epistaxis, dilated blood vessels, and arteriovenous malformations (9). Accordingly, in mice, inactivation of *Acvlr1* is lethal at midgestation due to severe vascular defects (10, 11).

BMP9 is mainly produced by the liver (12), whereas BMP10 is produced in embryos by the heart and in adults by the right atria (13). *Bmp10* deletion was first shown to lead to embryonic lethality due to cardiac defects (14). However, more recently, it was also shown that loss of *Bmp10* could also lead to vascular defects both in mouse and zebrafish (15, 16). On the other hand, *Bmp9* knockout (KO) mice are viable, but presented lymphatic defects (17). Interestingly, it was also found that BMP9 and BMP10 could compensate for each other's loss and that BMP9

[6] The abbreviations used are: BMP, bone morphogenetic protein; ALK, activin receptor-like kinase; BRE, BMP responsive element; cKO, conditional knock-out; CM, conditioned medium; ECM, extracellular matrix; FT, flow-through; HHT, hereditary hemorrhagic telangiectasia; HSC, hepatic stellate cells; HUVEC, human umbilical venous endothelial cell; HMVEC-d, human microvascular endothelial cells from the dermis; KO, knock-out; TGF, transforming growth factor.

and BMP10 play a redundant role in postnatal vascular development (15, 18, 19).

ELISAs have shown that human plasma contains both BMP9 (2–6 ng/ml) and BMP10 (0.5–2 ng/ml) (12, 15). It is widely admitted that BMP9 circulates under a biologically active form (7, 12), and functional and structural studies have confirmed that the binding of mature BMP9 to its prodomain does not prevent its binding to signaling receptors (12, 20, 21). However, there is still a debate about the latency of BMP10. First, it has been shown that, when bound to its prodomain, mature BMP10 is inactive (22), similarly to other members of the TGFβ family, including TGFβ (23) itself and myostatin (24). A more recent report indicates, however, that recombinant human BMP10 is fully active on endothelial cells, albeit it forms a very stable complex of the mature form associated with the prodomain (25). Along the same line, Chen *et al.* (15) have shown that anti-BMP10 antibodies could partially decrease Smad6 gene induction by mouse serum, indicating that active BMP10 is present in blood. These data thus appear in contradiction with the absence of ALK1-stimulating activity measured in *Bmp9*-KO mouse plasma (19). One hypothesis that could reconcile these results is that plasmatic ALK1 ligand is a BMP9–10 heterodimer rather than a mixture of homodimeric BMP9 and BMP10. Indeed, although most BMPs have been described as homodimeric proteins, they can also, to some extent, heterodimerize (1). Such heterodimers spark increasing interest because they likely provide a distinct signaling pattern (26).

The aim of the present work was to better characterize the circulating forms of BMP9 and BMP10 and to evaluate whether BMP9 and BMP10 can form a heterodimer. We provide evidence that, when co-expressed, BMP9 and BMP10 can associate to form a disulfide-bonded BMP9–10 heterodimer. More importantly, we identified the presence of BMP9–10 heterodimers in human and mouse plasma and show that this heterodimer is active and represents the major circulating form in blood.

Results

BMP9 and BMP10 can form heterodimers in vitro

To evaluate whether BMP9–10 heterodimerization can occur, we first transfected HEK-293 cells with both BMP9 and BMP10 cDNAs. First, we engineered recombinant BMP9 and BMP10 and added two different tags placed between the prodomain and the mature BMP peptide, *i.e.* downstream of the furin-cleavage site (Fig. 1*A*). BMP9 was tagged with a 6-histidine motif, whereas BMP10 was tagged with a myc epitope. Tagged BMP9 and BMP10 were transfected into HEK-293 cells, either solely or together and secreted BMPs were evaluated by Western blotting of conditioned media (CM) (Fig. 1*B*). Both BMPs were produced as incompletely processed molecules, as 3 bands around 110 kDa (unprocessed dimeric pro-BMP), 50–65 kDa (monomer or partially processed BMP), and 23 kDa (mature dimeric peptide) were revealed by Western blotting (Fig. 1*B*). To determine whether heterodimeric BMP9–10 could be produced by double-transfected cells, we affinity-purified the two BMPs using their specific tags. For this, CM from His-BMP9/myc-BMP10 co-transfected cells was applied onto a HisTrap^{TM} column and bound BMPs were then eluted and evaluated by Western blotting. As expected, His-BMP9 was fully retained by the HisTrap^{TM} column and only detected in the 200 mmol/liter of imidazole elution (Fig. 1*C*). Myc-BMP10 was partially detected in the unbound or weakly bound fractions (flow-through (FT), wash) but could also be observed in the elution fraction, demonstrating that BMP9 and BMP10 interacted when they were co-transfected (Fig. 1*C*). We then analyzed whether BMP9 and BMP10 could still interact under denaturing conditions. Under this condition, heterodimeric disulfide-bonded molecules should still co-elute, whereas oligomeric noncovalent BMP9–BMP10 complexes should be disrupted by denaturation. For this, CM was treated with 8 mol/liter of urea and heated for 20 min at 65 °C before being applied to the HisTrap^{TM} column. We observed that myc-BMP10 could still interact with His-BMP9 (Fig. 1*D*). On the contrary, further treatment resulting in reduction and alkylation of disulfide-bonds completely disrupted myc-BMP10 binding, as shown by the absence of signal in the eluate using an anti-myc antibody detection, albeit BMP9 was still detectable (Fig. 1*E*). As a control, loading of the HisTrap^{TM} column with single-transfected myc-BMP10 CM demonstrated the absence of non-specific binding of myc-BMP10 alone (Fig. S1).

To further support BMP9–10 heterodimerization, we generated unprocessed BMP variants by mutating amino acids in the furin-cleavage site, and we co-transfected mutated BMP9 with a wildtype (WT) BMP10 or vice versa. Heterodimerization of BMP9 and BMP10 was estimated by Western blotting as the association of a precursor and a mature BMP. For this, we removed the tags between the pro- and mature BMP domains. This enabled the full processing of pro-BMP9 and pro-BMP10, as shown by the single 23-kDa band revealed by Western blotting of CM issued from WT BMP9 or WT BMP10 single transfections (Fig. 1*F*). The BMP9 furin-cleavage site ^{316}RKKR was mutated to ^{316}RQKR, ^{316}RQAR^{319}, or ^{316}RQAA^{319}. The first mutant was generated to mimic a substitution mutation identified in a patient suffering from HHT (27). The two others replaced basic amino acids by alanine residues to avoid furin cleavage. The single substitution of Lys^{317} to Gln^{317} did not impair BMP9 maturation (Fig. S2), thus indicating that HHT disease in this patient is not linked to a BMP9 processing defect as it had been suggested (27). The double mutant RQAR was only partially processed but could be completely cleaved when furin was overexpressed, whereas the triple mutant RQAA was not cleaved at all even in the presence of overexpressed furin (Fig. S2). Similarly, BMP10 ^{313}RIRR^{316} sequence was mutated to RIAA. Fig. 1*F* shows that, similarly to the BMP9 RQAA mutant, the BMP10 RIAA mutant was exclusively expressed as a 110-kDa precursor. Thus, these mutations inhibit BMP processing and consequently, their capacity to activate ALK1 in a BRE assay using transfected 3T3 cells (7) (Fig. 1, *F* and *G*). Interestingly, co-transfection of the BMP10 RIAA mutant with WT BMP9 gave rise to a new 65-kDa BMP9 immune reactive band (*arrowhead*), likely corresponding to the association of mature WT BMP9 to BMP10 precursor. Similar results could be obtained with co-transfection of the BMP9 RQAA mutant together with WT BMP10 (Fig. 1*F*). These chimeric proteins (B9WT/B10 RIAA; B10 WT/B9 RQAA) were also unable to activate ALK1 in the BRE assay (Fig. 1*G*). This demonstrated a

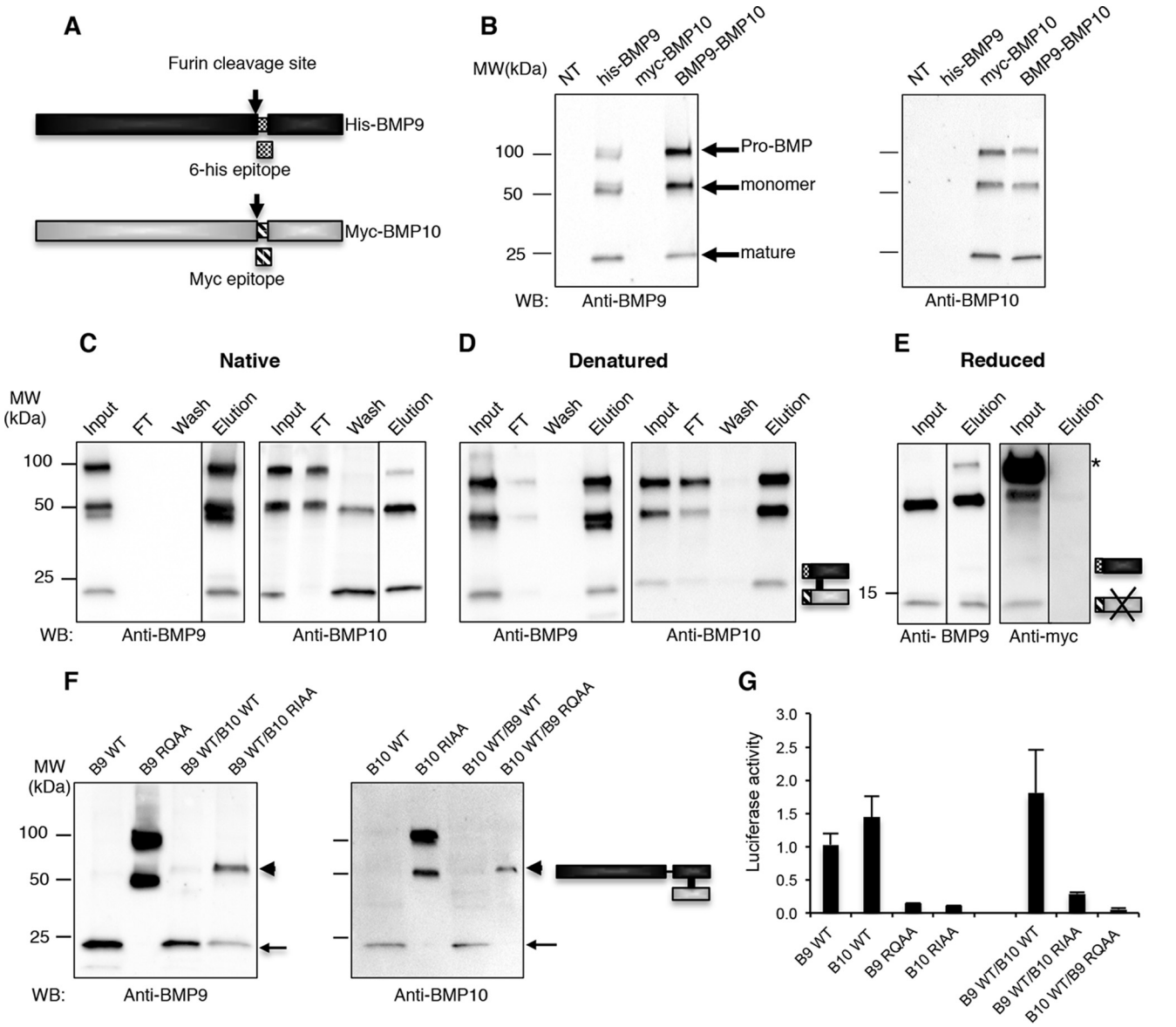

Figure 1. *A,* schematic representation of recombinant BMP9 and BMP10 (pro-BMPs), containing respectively a His_6 epitope and a myc epitope downstream of the furin-cleavage site. *B,* Western blot (*WB*) analysis of CM from HEK-293-transfected cells. HEK-293 cells were stably transfected with plasmids encoding His-BMP9, myc-BMP10, or both plasmids (indicated *BMP9–BMP10*). Proteins were detected with antibodies directed against the mature domain of BMP9 or BMP10 as indicated. All samples were run under non-reduced conditions. *NT,* nontransfected cells. *C–E,* HisTrap™ chromatography of CM from cells cotransfected with His-BMP9/myc-BMP10. *C,* CM applied under native conditions. *D,* CM denaturated by 8 mol/liter of urea and heated at 65°C for 20 min before being loaded onto the column. *E,* CM denatured as above, then reduced by DTT and alkylated before loading. Flow-through (*FT*) was collected. Columns were washed with 20 mmol/liter of imidazole (wash) and eluted by 200 mmol/liter of imidazole (elution). Fractions were analyzed by Western blot with the indicated antibodies under non-reduced (*C* and *D*) or reduced conditions (*E*). Note that the anti-myc antibody gives a strong non-specific band around 100 kDa (*). In *C* and *E*, elution tracks are surrounded by a *black line* to highlight spliced 10 mM imidazole washing fractions. *F* and *G*, heterodimerization of a mutant BMP and a wildtype (*WT*) counterpart. Fully-cleaved mature WT BMP9 and BMP10 have been produced without any tag sequence. BMP9 and BMP10 furin-cleavage sites have been mutated to create uncleavable sequences, respectively, RQAA and RIAA. Wildtype and mutant BMPs have been solely transfected (0.5 ng of plasmid in each condition), or co-transfected (0.5 ng of plasmid coding for WT BMP and 1.5 ng of mutant BMP) into HEK-293 cells. CM were analyzed by Western blotting with the indicated antibodies directed against mature BMPs (*F*) or for their BRE activity on ALK1-transfected 3T3 cells (*G*). *Arrows* in *F* show the bands corresponding to mature BMPs. *Arrowheads* point to a 65-kDa band resulting from the dimerization of a wildtype BMP and a mutant pro-BMP. In *G*, co-transfection with a mutant BMP leads to a dominant-negative effect on ALK1–BRE stimulation. Values represent relative firefly luciferase normalized to *Renilla* luciferase activity.

dominant-negative effect of the mutant BMP on the activity of WT BMP9 or -10. Altogether, these results support that BMP9 and BMP10 form a disulfide-bonded heterodimer when coexpressed in the same cells.

BMP9–10 heterodimer is biologically active

BMP9–10 heterodimers were purified in two steps using a HisTrap™ column followed by an affinity column grafted with anti-myc antibodies. The latter allowed separating His-BMP9 homodimers from BMP9–10 heterodimers. Elution was performed by lowering the pH to 3 (fraction containing mainly BMP9) and then to 2 (fraction containing BMP9–10 heterodimer) (Fig. S3). The mature BMP9–10 heterodimer was carefully quantified by Western blotting using known quantities of commercial BMP9 and BMP10 as standards under reduced (BMP9) or unreduced (BMP10) conditions (see

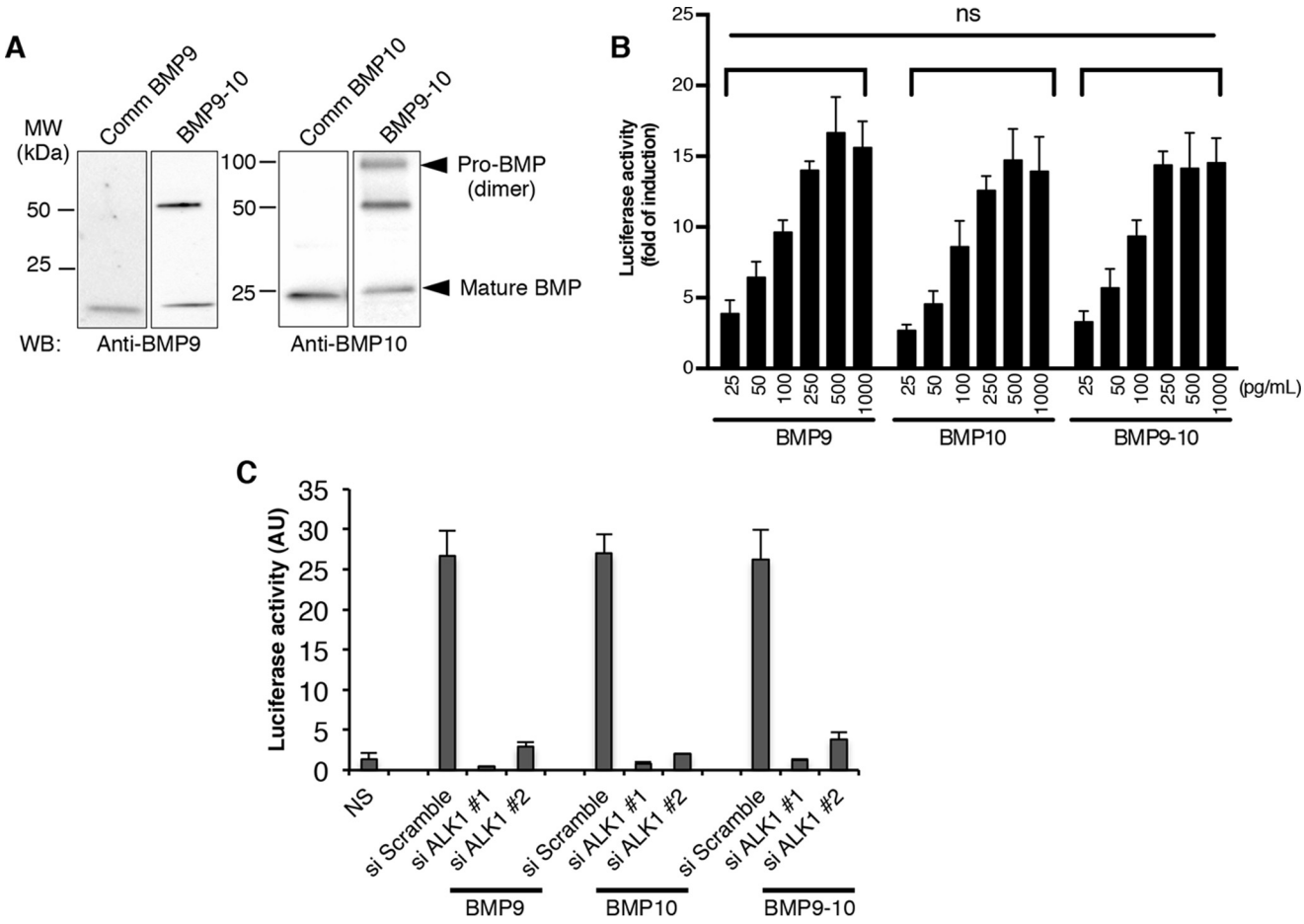

Figure 2. Recombinant BMP9–10 heterodimer is active on endothelial cells through the ALK1 receptor. *A,* Western blotting (*WB*) detection of purified BMP9–10 heterodimer under reduced (*BMP9*) or unreduced (*BMP10*) conditions. BMP9–10 was purified through a HisTrap™ column followed by a anti-myc-agarose column and bound heterodimer was eluted by glycine, pH 2 (see Fig. S3). BMP9–10 was quantified using Image Lab (Bio-Rad) after Western blotting. Band intensity was measured on the mature form (23 and 14 kDa for nonreduced or reduced, respectively) and compared with known amount of commercial (*comm*) BMP9 or BMP10. The figure shows lanes with 5 ng of each BMP. *B,* HUVECs were transfected with pGL3(BRE)2-luc and pRL-TK-luc and stimulated with BMP ligands in a range from 25 to 1000 pg/ml. Results show the fold-induction over control unstimulated cells. Data are the mean ± S.E. of 4 independent experiments conducted in duplicate. For each dose, statistical analysis was performed and indicated no significant difference between the 3 ligands (two-way analysis of variance multiple comparison test followed by a Tukey post test). *C,* HUVECs were transfected with duplex siRNA (scramble *versus* two different ALK1 siRNA) and further transfected 48 h later with pGL3(BRE)2-luc and pRL-TK-luc. They were then stimulated with 250 pg/ml of ligands and results are expressed as the fold-induction over nonstimulated cells (*NS*). The figure shows one representative experiment out of two conducted in duplicates.

Fig. 2*A*). The activity of BMP9–10 heterodimer was then determined on human umbilical venous endothelial cells (HUVECs) transfected with the BRE-luc reporter plasmid. The BMP9–10 heterodimer displayed a similar stimulation pattern than BMP9 or BMP10 homodimer: induction started with low doses of ligand (25 pg/ml) and a plateau was obtained at doses higher than 250 pg/ml (Fig. 2*B*).

We next addressed whether the activity of the BMP9–10 heterodimer was mediated by ALK1 signaling. To do this, we knocked down ALK1 expression by transfecting HUVECs with two different siRNA specific for ACVLR1. The activity of BMP9, BMP10, and BMP9–10 was then evaluated as above, using the BRE-luc reporter. The activities of BMP9, BMP10, and BMP9–10 were completely (siRNA#1) or severely (siRNA#2) abolished compared with transfection with scramble siRNA (Fig. 2*C*). The loss of activity was correlated with the level of ACVLR1 gene extinction (Fig. S4*A*). Moreover, we also found that BMP9, BMP10, and BMP9–10 lost their ability to induce the phosphorylation of Smad1–5, indicating that ALK1 is necessary for activating the Smad pathway in a similar way for the 3 ligands (Fig. S4*B*).

BMP9–10 heterodimer is present in mouse plasma and is the main active circulating form

To quantify BMP9–10 heterodimers, we set-up a cross-ELISA, using a capture anti-BMP9 antibody and a detection anti-BMP10 antibody, or the other way round, *i.e.* a capture anti-BMP10 antibody and a detection anti-BMP9 antibody. We compared their immune reactivities with those of standard BMP9 (12) and BMP10 ELISAs (R&D Systems). BMP9 and BMP10 ELISAs both specifically recognized homodimeric BMP9 or BMP10, respectively, but also allowed the detection of purified BMP9–10 heterodimer (Fig. S5, *A* and *B*). On the contrary, cross-BMP9–10 or cross-BMP10–9 ELISAs specifically only detected purified BMP9–10 heterodimers but not BMP9 or BMP10 homodimers (Fig. S5, *C* and *D*). Moreover, CM containing a mixture of BMP9 and BMP10 gave no signal, demonstrating that only disulfide-bonded heterodimer is recog-

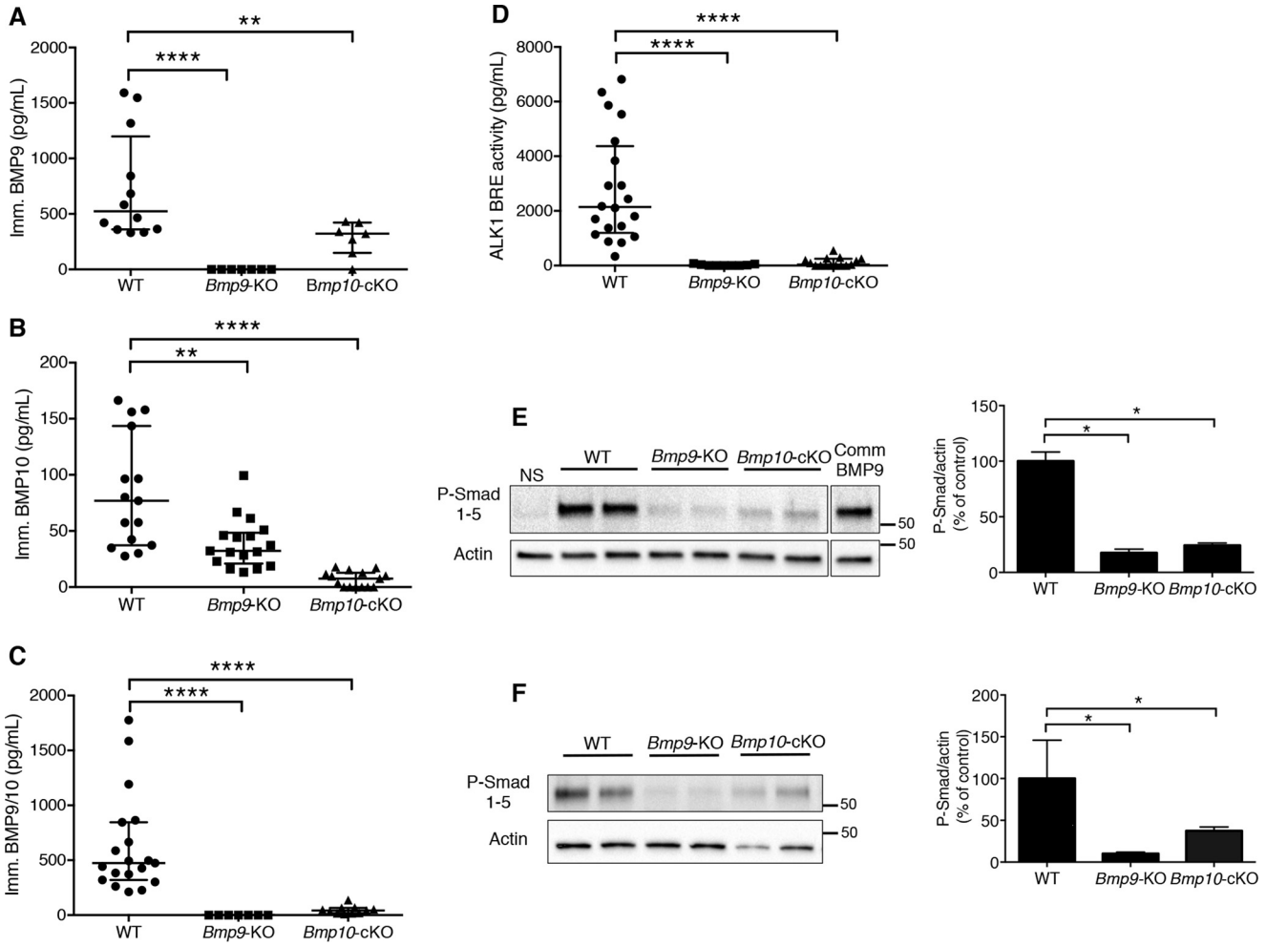

Figure 3. BMP9–10 heterodimer is present in mouse plasma and is the only active ALK1-stimulating form. *A–C*, ELISA measurements of circulating BMP9 (*A*), BMP10 (*B*), or BMP9–10 heterodimer (*C*) in plasma from WT, *Bmp9*-KO mice, and *Bmp10*-cKO mice. BMP9–10 ELISA was realized using a capture antibody against mature BMP9 and a detection antibody against BMP10. Recombinant BMP9 and BMP10 or purified BMP9–10 heterodimer were used as standards. $n = 7$ to 15 mice. Results are presented as the median ± interquartile range (*Imm*) of BMP immune reactive BMP. *D*, ALK1–BRE activity of plasma from WT, *Bmp9*-KO, and *Bmp10*-cKO mice using a BRE assay on 3T3-transfected cells. Values are presented as mean ± S.E. from 8 to 15 mice. *E* and *F*, immunoblotting of primary human endothelial cell lysates (*E*, HMVEC-ds; *F*, HUVECs) using phospho-Smad1–5 antibody. Cells were starved for 90 min and stimulated for 20 min with 3% plasma from WT, *Bmp9*-KO, or *Bmp10*-cKO mice. Blots show 2 different mice per condition. The position of the 50-kDa marker is indicated by the *line on the right* of each blot. Stimulation values were normalized to actin expression and represented as the % of stimulation with WT plasma taken as 100% (mean ± S.E.). Quantification has been made on 4 different mice for each condition. Stimulation with 100 pg/ml of commercial BMP9 under the same conditions is shown as a control in *E*. Statistical comparison of KO-mice *versus* WT mice was performed using a Mann-Whitney test: *, $p < 0.05$; **, $p < 0.01$; ****, $p < 0.0001$.

nized by these cross-ELISAs. Standard curves using purified BMP9–10 could be established and showed a sensitivity threshold around 30 pg/ml for both cross-ELISAs (Fig. S5, *E* and *F*).

We then sought for the presence of heterodimeric BMP9–10 in mouse plasma. We took advantage of comparing WT and KO mice in which *Bmp9* (19) or *Bmp10* have been genetically invalidated. As *Bmp10*-KO is embryonic lethal, we generated conditional KO mice by crossing *Bmp10*-floxed mice with Rosa26-CreER^{T2} mice (28). Deletion of *Bmp10* was performed in 3-week-old mice by daily injection of tamoxifen for 5 days. *Bmp10* knock-down efficiency was evaluated by RT-qualitative PCR on the right atria, 6 weeks after tamoxifen injection. A very strong, although not complete reduction in BMP10 levels was observed (Fig. S6*A*). *Bmp10* deletion was also checked by measuring the ALK1–BRE activity from protein extracts of the right atria. In accordance with the mRNA levels, only 10% of ALK1–BRE activity remained 3 weeks after tamoxifen injections (Fig. S6*B*). Following *Bmp10* deletion, mice were viable and did not display any obvious phenotype. We next measured the homo- and heterodimeric BMP9/10 species by ELISA. The results are presented as the immune reactivity as it is difficult to give the accurate concentrations of circulating BMP using ELISA: we are using mature recombinant proteins as standards but BMPs circulate under different forms (uncleaved, processed, and complexed) and we know that the antibodies might not recognize the different forms of BMPs with the same affinity (12, 29).

As expected, BMP9 and BMP10 were detected in WT plasma (Fig. 3, *A* and *B*), but very interestingly, using a cross-BMP9–10 ELISA, we also found the presence of BMP9–10 heterodimers in WT plasma (Fig. 3*C*). Furthermore, BMP9–10 heterodimer was no more detected in the plasma of *Bmp9*-KO mice, and its level was also strongly reduced in *Bmp10*-cKO *versus* WT mice (Fig. 3*C*). This slight remaining level of heterodimer in *Bmp10*-

cKO plasma is likely due to the incomplete knockdown of *Bmp10* expression (Fig. S5, *A* and *B*) as circulating BMP10, measured by ELISA, was also not completely suppressed (10% residual immune reactivity) (Fig. 3*B*). Interestingly, we also observed a strong decrease in BMP9 levels in the plasma of *Bmp10*-cKO mice (Fig. 3*A*), supporting that a large part of BMP9 immune reactivity can be attributed to the BMP9–10 heterodimer. Similarly, we found a significant decrease in BMP10 levels in the plasma of *Bmp9*-KO mice (Fig. 3*B*), likely due to the loss of BMP9–10 heterodimers. It is worth noting that the BMP10 ELISA detected much lower levels of circulating BMP10 than BMP9–10 heterodimers, suggesting an epitope detection problem for BMP10 from blood with the BMP10 ELISA (Fig. 3, *B* and *C*).

We next evaluated the ALK1 stimulating activity of these plasma using the ALK1–BRE assay. As previously described (19), no ALK1–BRE activity could be detected in *Bmp9*-KO plasma but interestingly, 90% of ALK1-stimulating activity was also lost in the plasma of *Bmp10*-cKO mice (Fig. 3*D*). To confirm the loss of activity from these plasma, we analyzed their ability to activate Smad1–5 phosphorylation in human endothelial cells. This was done either on human microvascular endothelial cells from the dermis (HMVEC-ds) (Fig. 3*E*) or HUVECs (Fig. 3*F*). WT plasma induced a strong Smad1–5 phosphorylation in both endothelial cell types, whereas plasma from both KO mice were hardly able to induce Smad1–5 phosphorylation. These results confirm that most of the circulating stimulating activity is lost when either *Bmp9* or *Bmp10* expression is knocked down. It is worth noting that the right atria of *Bmp9*-KO mice still expressed active BMP10 ligand, as shown by the high specific activity of protein extracts from the right atria similar to that of WT mice and that this activity could be fully inhibited by anti-BMP10 antibodies (Fig. S6*C*). Therefore, cardiac BMP10 is normally synthesized and active, even in the absence of BMP9 expression.

Taken together these data show for the first time the presence of a BMP9–10 heterodimer in mouse plasma. The loss of plasmatic activity both in *Bmp9*-KO mice and *Bmp10*-cKO mice strongly supports that this activity is due to the BMP9–10 heterodimeric form as otherwise we would have been able to detect the BMP10 activity in *Bmp9*-KO plasma and vice versa a BMP9 activity in *Bmp10*-cKO plasma.

BMP9–10 heterodimer circulates as an active ligand in human plasma

We then tried to detect BMP9–10 heterodimers in human plasma using the BMP9–10 crossed ELISA that we have set-up (Fig. S5, *E* and *F*). 19 plasmas from healthy individuals were measured. Very interestingly, we found circulating BMP9–10 heterodimers in human plasma (Fig. 4*A*).

To further support our data, we undertook the characterization of BMP9–10 heterodimers from human plasma by affinity chromatography on anti-BMP10 antibodies. For this, we passed a pool of human plasma (10 ml) through an affinity chromatography column grafted with anti-BMP10 antibodies and eluted bound BMPs by acidic pH. ELISAs and ALK1–BRE assays were then performed on the flow-through (FT) and elution fractions. The data are expressed as the quantity of each BMP recovered

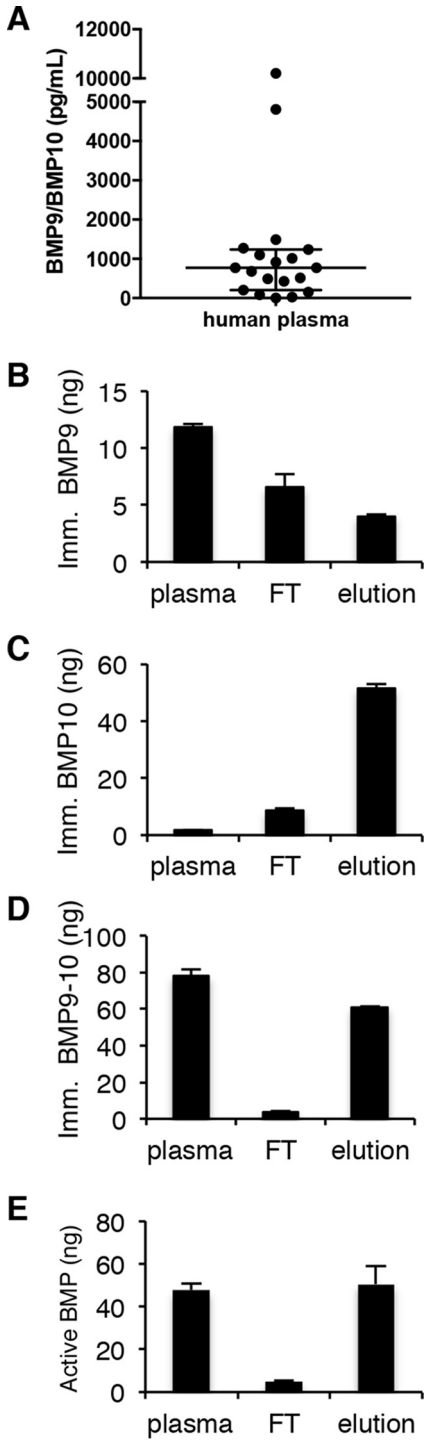

Figure 4. BMP9–10 heterodimer is present in human plasma and is the main ALK1-stimulating form. *A,* quantification of BMP9–10 heterodimer in 19 healthy human plasma. BMP9–10 ELISA was realized using a capture antibody against mature BMP10 and a detection antibody against BMP9. Results are presented as the median ± interquartile range (*Imm*). *B–E,* purification and activity of BMP9–10 heterodimer from human plasma. BMP9–10 heterodimer was purified by affinity chromatography: 10 ml of a pool of human plasma (selected for its high BMP9–10 immune reactivity, 8–10 ng/ml) was applied to an anti-BMP10 column, and eluted by glycine, pH 2.7. *B–D,* ELISAs: plasma, FT, and elution fractions were quantified by ELISA to detect BMP9 (*B*), BMP10 (*C*), or BMP9–10 heterodimer under the same conditions as in *A* (*D*). *y* axes represent the total amount of immune reactive BMP9, BMP10, or BMP9–10. *E,* ALK1–BRE activity of the different fractions was measured on 3T3 cells. Recombinant BMP9 was used as a standard to quantify the total amount of active BMP in each fraction. Values are the mean ± S.D. of duplicates measured by ELISA or BRE-luc assay from one representative experiment out of 3.

in each fraction. The FT fraction contained mostly BMP9 homodimers (Fig. 4*B*) and low levels of BMP10 homodimers (Fig. 4*C*) as nearly no BMP9–10 was detected (Fig. 4*D*). Interestingly, BMP9–10 was highly recovered in the elution fraction, as measured by the BMP9–10-crossed ELISA further supporting the presence of a BMP9–10 heterodimer in human plasma (Fig. 4*D*). Surprisingly, more BMP10 epitopes could be detected in the FT and elution fractions than in the whole plasma (Fig. 4*D*), suggesting the presence of masking proteins in plasma impending BMP10 measurement as already suggested in murine plasma (Fig. 3*B*). As a similar amount of immune reactive BMP10 and BMP9–10 is detected in the eluate, this suggests that BMP10 ELISA can detect BMP9–10 heterodimer in this fraction, whereas it could not in plasma.

Interestingly, most of the ALK1–BRE activity was detected in the elution fraction that contained the BMP9–10 heterodimer (Fig. 4*E*). The FT, containing mostly homodimeric BMP9, was not very active. Altogether, these data demonstrate that, similarly to mouse plasma, BMP9–10 heterodimer is the major ALK1 activator circulating in human plasma.

Hepatic stellate cells synthesize BMP9 and BMP10

Heterodimeric BMP9–10 bonding implies that BMP9 and BMP10 are produced by a common cell type. We previously described, using mRNAs from 20 human tissues (Clontech), that BMP9 mRNA is mostly expressed by the liver (12). Using the same samples, we measured BMP10 mRNA expression. We found that BMP10 was, as expected, mostly expressed in the heart but also, although at a lower level, in liver (Fig. 5*A*). We thus hypothesized that liver could be the organ responsible for the expression of circulating BMP9–10 heterodimer. We used the RNAscope technology to identify BMP9- and BMP10-producing cells in mouse liver sections. The BMP10 probe was first validated on mouse adult heart cross-sections. As expected, a strong pink labeling was specifically observed in the right atria, whereas the ventricle was completely negative (Fig. 5*B*). No BMP9 mRNA expression could be detected in the heart (Fig. 5*B*). On the contrary, liver sections showed BMP9-positive cells throughout the liver lobules (Fig. 5*C*). Higher magnification indicated that positive cells were triangular stellate-shaped cells, spread between hepatocytes and sinusoids, having a typical morphology of hepatic stellate cells (HSCs). No staining was observed in other hepatic cells, *i.e.* hepatocytes, sinusoidal endothelial cells, or Kupffer cells (Fig. 5*C*). Interestingly, BMP10 staining, albeit weaker than BMP9 staining, was also specifically observed in HSCs (Fig. 5*C*). As expected, BMP9 and BMP10 staining were lost in the respective *Bmp9*-KO, and *Bmp10*-cKO liver sections (Fig. S7), demonstrating the specificity of the labeling. BMP10 staining was still observed in liver from *Bmp9*-KO, and vice versa, supporting that BMP9 and BMP10 do not regulate the expression of each other. From this, we conclude that HSCs can synthesize both BMP9 and BMP10 and could be the physiological source of BMP9–10 heterodimer.

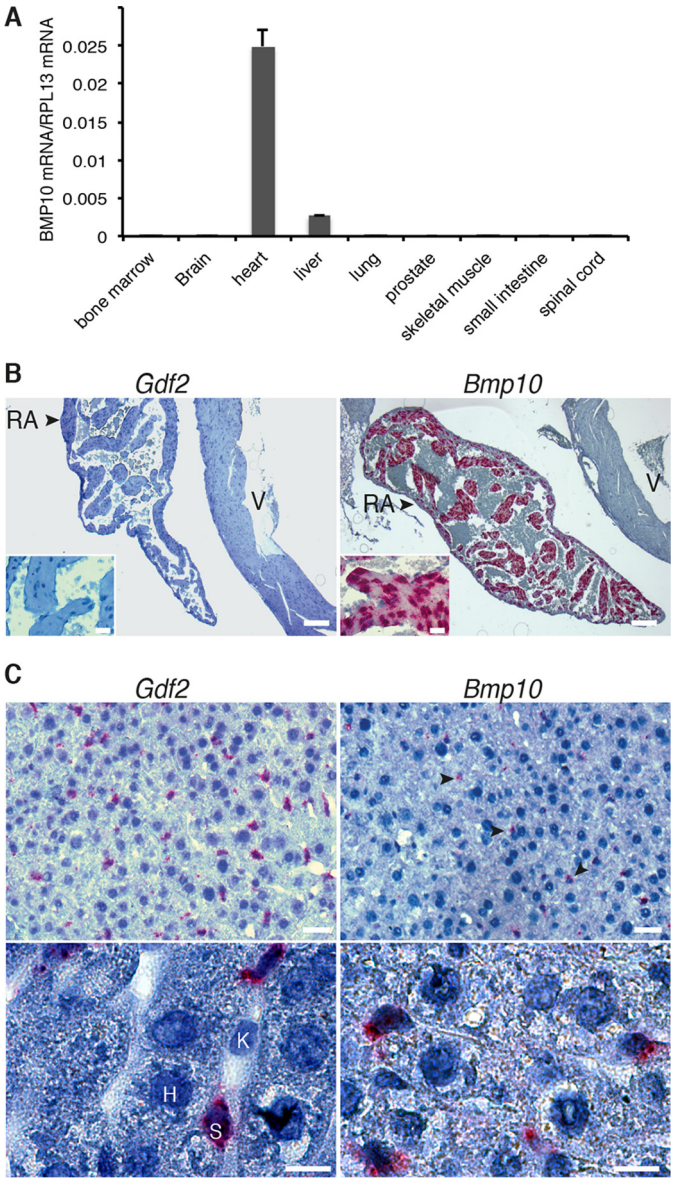

Figure 5. Hepatic stellate cells synthesize both BMP9 and BMP10. *A,* Bmp10 mRNA expression in human tissues (Clontech, 9 tissues out of 20 analyzed) determined by quantitative RT-PCR. Results are shown as the mean ± S.D. of Bmp10 mRNA level normalized to RPL13 mRNA levels. *B* and *C,* localization of Gdf2 (Bmp9) or Bmp10 mRNA by RNAscope on mouse adult heart sections (*B*) or liver sections (*C*). Paraffin-embedded sections were labeled with *Gdf2* probe for BMP9 (*left panels*) or *Bmp10* probe (*right panel*) revealed by fast-red pink staining and counterstained with hematoxylin. In *B,* right atria (*RA*), ventricle (*V*). *Insets* show higher magnification of the right atria (*scale bar*, 25 μm). In *C, upper panels* show low magnification with several positive pink cells (*arrowheads*). *Lower panels* are high magnifications showing hepatocytes (*H*), a Kupffer cell (*K*), lining the wall of a sinusoid and stellate cells (*S*) between hepatocytes and sinusoids. Note the pink labeling of stellate cells.

Discussion

Our work demonstrates for the first time that BMP9 and BMP10, two BMPs from the same subfamily, which share 65% protein sequence identity, can heterodimerize by disulfide bonding in the C-terminal mature domain to produce an active BMP9–10 heterodimer. It also shows that this heterodimer is present in both human and mouse plasma, and that this circulating form is the main entity capable of activating the endothelial receptor ALK1 both in 3T3-transfected cells and in primary endothelial cells.

Most TGFβs and BMPs have been described as homodimeric proteins, but several reports demonstrate that they can also, to some extent, heterodimerize (1). The recently established

structures of pro-TGβ1, pro-activin A, and pro-BMP9 support that arm domain-growth factor domain swapping could provide a mechanism for preferential formation of heterodimers over homodimers when a cell synthesizes monomers of two different TGF-β family members (30). Heterodimeric BMPs, including BMP2–BMP7, BMP4–BMP7, and BMP2–BMP6, have been shown to play critical roles in embryonic development in various organisms including *Drosophila* (31, 32), zebrafish (33), *Xenopus* (34), and mammals (35). Nodal–GDF1 heterodimers have also been shown to be involved in left-right patterning (36, 37). There is, however, only little evidence of the expression of these heterodimers in adults. One example is illustrated by the discovery of cumulin, a GDF9–BMP15 heterodimer, which is an oocyte-specific growth factor involved in granulosa cell differentiation and a key regulator of ovarian function (38, 39). In the present work, we identify a new heterodimeric BMP ligand, BMP9–10, which is circulating in adult blood and is likely a key factor for blood vessel homeostasis. To measure its circulating levels, we have set-up a cross-ELISA that specifically recognizes heterodimeric BMP9–10 and does not cross-react with the homodimeric forms. To our knowledge, this is the first time that BMP heterodimers can be quantified from *in vivo* sources. This original approach of cross-ELISA could be developed in the future for other BMPs to more generally assess the occurrence of BMP heterodimers in tissues.

Our previous work on *Bmp9*-KO mice showed no ALK1-stimulating activity in the plasma of these mice. We therefore proposed that circulating BMP9 was the main active ALK1 ligand in blood (19). In the present report, we show that *Bmp10*-cKO mice have also lost most of their circulating ALK1-stimulating activity on 3T3-transfected cells. More importantly, plasma devoid of BMP9 or BMP10 failed to activate P-Smad1–5 on endothelial cells, indicating that BMP9–10 is the only active ligand in blood. It might thus be surprising that *Bmp9*-KO mice are viable and healthy and that they do not present any obvious blood vessel developmental defects as well as *Bmp10*-cKO when deleted in adult mice. One hypothesis that would support our data are that latent homodimeric BMP9 or -10 are still present, albeit not detected in plasma, which can still be locally activated. Along this line, recent structural data of the pro-BMP complex showed that pro-BMP9 can adopt both cross-armed and open-armed conformations, which could correspond to latent and nonlatent states, respectively (21). The transition between the two states could be regulated through the binding to ECM proteins, acting as BMP reservoir (22, 40). Such ECM interactions have been recently demonstrated for the BMP7–prodomain complex, which when bound to fibrillin-1 confers a "closed arm" conformation and denies access of BMP receptors to the growth factor (41). Because BMP10 prodomain has been shown to also bind fibrillin (42), we can envision that such a mechanism could also occur for BMP9 and BMP10 homodimers.

Most heterodimeric BMPs, when produced as recombinant proteins, usually show an increased activity, as compared with their homodimeric counterparts (43–46). It is admitted that the high potency of heterodimers is due to their increased versatility regarding receptor binding. Indeed, heterodimers often consist of the association of a member of the BMP2/4 subgroup, having a high affinity to type I receptor, but a low affinity to type II receptors (47) and a member of the BMP5/6/7/8/8b subgroup, having a higher affinity to type II receptors than to type I receptors (48). The combination of both would then enhance the global affinity for the receptor complex. To this respect, BMP2–6 heterodimer displays high affinity for both type I and type II receptors (44). Moreover, heterodimeric association could induce the recruitment of two different type I receptors in the same signaling complex, thus inducing a stronger and/or distinct downstream signaling (44). Such a mechanism has been elegantly demonstrated in the zebrafish embryo, where the signaling by BMP2–7 induces a synergistic activity of ALK3 and ALK6, which is required for dorsoventral patterning (33).

In contrast to these studies, in our assays, the BMP9–10 heterodimer did not display any higher activity than its homodimeric counterparts. The BMP9–10 heterodimer has, however, only been challenged on endothelial cells expressing the ALK1 receptor. ALK1 is a type I receptor of very high affinity (K_d = 2 pM), explained by a unique receptor orientation toward its ligands that is distinct from the other type I receptors (49, 50). ALK1 has a similar affinity for BMP9 and BMP10 and is stimulated with very low concentrations of ligand (as low as 25 pg/ml). To this regard, it might not be surprising that the BMP9–10 heterodimer displays the same activation pattern as BMP9 and BMP10 homodimers. It may be possible that this heterodimer differentially activates cells that do not express ALK1. Indeed, BMP9 and BMP10 present differential affinities toward the three type II receptors (50) and the initial binding of the BMP9–10 heterodimer to a given subset of type II receptors might allow the subsequent recruitment of a lower affinity type I receptor such as ALK2 or ALK3. BMP9 has been shown to signal through ALK2 (51, 52) and BMP10 through ALK3 (53) in nonendothelial cell types. It is tempting to speculate that BMP9–10 heterodimer could drive a specific signal through this receptor set and further work is needed to characterize ALK1-independent cellular responses. However, one has to keep in mind that not all heterodimers produce a synergistic signal due to the recruitment of different receptors. In *Drosophila*, the Dpp/Gbb heterodimer does not lead to a stronger signal but its more effective signaling is attributed to its better transport (54). Hence, specific binding and cleavage play essential roles in spatial regulation of the BMPs activity, as shown in embryonic patterning and vein development with Dpp/Scw heterodimer in *Drosophilia* (1, 31, 32). Heterodimerization of BMP9 and BMP10 could lead to a differential localization than homodimers.

Biosynthesis of disulfide-bonded heterodimeric BMPs supposes a common production site for both BMPs. Analysis of BMP10 mRNA expression in 20 different tissues confirmed that BMP10 was mostly expressed by the heart but that some BMP10 expression could also be found in liver (Fig. 5*A*). Using the powerful RNAscope technology, we found that BMP9 and to a lower extent BMP10 mRNAs are present in HSCs. The source of BMP9 expression has been debated for a long time (12, 55), but HSCs have been recently described as the cellular source for BMP9 protein (56), in agreement with mRNA detection in the present work (Fig. 5*C*). We propose that HSCs could be the cells that produce the BMP9–10 heterodimer but further

experiments with isolated primary HSCs are needed to confirm this hypothesis.

The ALK1-stimulating activity in the right atria is significantly decreased in *Bmp10*-cKO mice but not in *Bmp9*-KO mice (Fig. S5). This supports the hypothesis that the heart only produces BMP10 homodimer and that this homodimer is not secreted into the circulation, or its activity negatively regulated because no circulating activity is found in *Bmp9*-KO mice.

Taken together, our results open a new field of investigation for BMP heterodimers, as we show for the first time the presence of a BMP9–10 heterodimer in the plasma of adult humans and mice. Which additional functions are triggered by this circulating heterodimer that its homodimeric counterparts do not fulfill is still an open question and will require further studies in cellular contexts where various combinations of type I and type II receptors are expressed. Which mechanisms control the differential synthesis and bioavailability of BMP9 and BMP10 homo- and heterodimers in liver and heart is also an intriguing question to be addressed in the future.

Experimental procedures

BMP9 and BMP10 recombinant expression and purification

Human full-length BMP9 and BMP10 were, respectively, cloned into pCEP4 vector or pcDNA3.1 zeo vector (Thermo Fisher Scientific, Waltham, MA). An additional sequence was inserted between the prodomain and the mature region for specific tagging of each BMP: a 6-histidine motif for BMP9 or a myc epitope for BMP10. BMP9 and BMP10 were also generated without tags and used as templates to create mutants in the furin-cleavage site of each BMP through site-directed mutagenesis using the Stratagene QuikChange kit (BMP9: R317Q,K318A,K319A; BMP10: R315A,R316A). All vectors and mutants were verified by DNA sequencing.

Constructs were transfected in HEK-293–EBNA cells using Lipofectamine 2000. Transfected cells were selected using the appropriate antibiotics (300 μg/ml of hygromycin for PCEP4–BMP9, 200 μg/ml of zeocin for pcDNA3–BMP10) and screened for protein expression by Western blotting of serum-free CM using anti-BMP9 (kind gift of Dr. Yan, Genentech, South San Francisco, CA) or anti-BMP10 (MAB2926, R&D Systems, Abingdon, UK).

For purification of BMP9–10 heterodimer, 200–500 ml of CM were dialyzed against 50 mmol/liters of sodium phosphate buffer, pH 8.0, and applied onto a HisTrap^{TM} column (GE Healthcare, Little Chalfont, UK). Columns were washed with 10 and 20 mmol/liters of imidazole and eluted with 200 mmol/liters of imidazole in phosphate buffer. In some cases, CM was first denaturated by dialysis against 8 mol/liter of urea, or alternatively by 1% SDS, followed by 20 min heating at 65 °C. CM could even undergo a further reduction step with 10 mmol/liter of DTT followed by alkylation of reduced cysteines by 25 mmol/liter of iodoacetamide. DTT was then removed by dialysis before loading CM onto the column.

HisTrap^{TM} eluates were further purified by affinity chromatography on anti-c-myc-agarose (Thermo Fisher Scientific). Samples were loaded in PBS, Tween 20, 0.1%, extensively washed with the same buffer and sequentially eluted by 0.1 mol/liter of glycine at pH 3 then pH 2. BMP9 and BMP10 were quantified in all fractions by Western blotting with anti-mature BMP9 (kind gift of Genentech, San Francisco, CA) and BMP10 (clone 13C11, homemade mAb previously used in Ref. 18 using commercial recombinant BMP9 or −10 (R&D Systems) as standard (1–10 ng/lane). The quantity of purified BMP9–10 heterodimer was calculated from the 23-kDa (BMP10, unreduced) or 14-kDa (BMP9, reduced) immune-reactive bands. Band intensities were quantified using Image Lab software (Bio-Rad).

Anti-BMP10 Ab-affinity purification of human plasma

Anti-BMP10 antibody (clone 13C11, see above) was coupled to NHS-activated Sepharose (2 mg/ml of resin) using standard protocols (GE Healthcare). 10–30 ml of human plasma (Biopredic International, pool of donors) was diluted 1:1 in PBS and applied to the column using an Äkta chromatography system. The column was washed with phosphate buffer containing 0.5 mol/liter of NaCl, and eluted by glycine-HCl, pH 2.7.

Bmp9- and Bmp10-KO mice

The generation of *Bmp9*-KO mice was described previously (19). To circumvent the early embryonic lethality of *Bmp10*-KO mice (14), the Institut Clinique de la Souris (Illkirch, France) generated a *Bmp10*$^{lox/lox}$ mouse by flanking *lox*P sites around exon 2. These mice were then crossed with Rosa26-CreER^{T2} mice provided by Prof. P. Chambon (IGBMC, Illkirch, France) (28) to generate conditional KO of *Bmp10* (*Bmp10*-cKO mice). Intraperitoneal injections of tamoxifen (1 mg) were performed for 5 days in 3-week-old mice. Blood was collected 6 weeks later on EDTA tubes. Plasma were obtained by centrifugation at 2000 × *g* for 10 min. All animal studies were approved by the institutional guidelines and those formulated by the European Community for the Use of Experimental Animals. *Bmp9*-KO and *Bmp10*-cKO mice were viable. They were maintained in the C57/BL/6 background.

Right atria extracts

Right atria were retrieved from 1–2-month-old mice. Tissues were homogenized in 50 mmol/liter of Tris-HCl, pH 7.4, 0.5 mol/liter of NaCl in the presence of a mixture of proteases inhibitors (Sigma) with a MagNA Lyser (Roche Diagnostics, Meylan, France).

Cell culture, transfection, and dual luciferase activity assay,

NIH-3T3 cells were transfected with a mixture of the reporter plasmid pGL3(BRE)2-luc encoding firefly luciferase downstream of a BMP response element, pRL-TK luc encoding *Renilla* luciferase and a plasmid encoding human ALK1, as previously described (7).

HUVECs were grown in EGM-2 (Lonza, Basel, Switzerland) and transfected by pGL3(BRE)2-luc and pRL-TK-luc in the absence of serum with Lipofectamine 3000 accordingly to the recommended protocols (Thermo Fisher Scientific). Cells were stimulated 2 h after transfection and lysed after 6 h for luciferase assay measurement.

To analyze Smad1–5 phosphorylation, HUVEC or HMVEC-d cells (Lonza) were starved for 90 min in EBM-2 without serum and

supplements, and stimulated for 20 or 30 min with the indicated ligands. Cells were then lysed and phospho-Smads were detected by immunoblotting with rabbit anti-P-Smad1–5 (Cell Signaling, Danvers, MA) (57).

HUVECs were transfected with Silencer® Select siRNA (s986, s987, scramble, Thermo Fisher Scientific) with RNAi max Lipofectamine using the recommended protocols. Cells were used 48 h later and transfected by pGL3(BRE)2-luc and pRL-TK luc as above. The extinction efficiency of ALK1 expression was evaluated by quantitative RT-PCR.

Enzyme-linked immunosorbent assay (ELISA)

BMP10 ELISA was performed with a commercially available assay (R&D Systems) that recognizes both human and mouse mature BMP10. This ELISA was different from the one previously used (19), and gave more reliable results. BMP9 and heterodimeric BMP9–10 ELISA measurements were performed as follows. 96-Well microplates were coated with the capture antibody: MAB3209 (R&D Systems) for BMP9, $^{13}C_{11}$ for BMP10, and incubated overnight at room temperature. After blocking with 5% BSA in PBS, all samples except plasmas were diluted in PBS containing 1% BSA, 0.1% Tween 20, added into the wells, and incubated for 2 h at room temperature. Plasma samples were diluted in PBS, 0.05% Tween 20, 0.5% Triton X-100. Biotinylated detection antibodies (anti-mature BMP9: BAF3209, R&D Systems or anti-mature BMP10: DuoSet R&D Systems, DY2926) were incubated for 2 h at room temperature. Plates were then revealed and read at 450 nm. Standard curves (15–1000 pg/ml) were obtained with recombinant BMP9 and BMP10 (R&D Systems) or purified BMP9–10 that had been quantified by Western blotting.

Quantitative RT-PCR

RNAs were extracted, and reverse-transcribed as previously described (19). Real-time PCR was performed using Bio-Rad CFX with the specific mouse *Bmp10* primer: forward, 5′-TCCATGCCGTCTGCTAACATCATC-3′, reverse, ACATCATGCGATCTCTCTGCACCA, and RPL13: forward, 5′-CCCTCCACCCTATGACAAGA-3′, reverse, 5′-TTCTCCTCCAGAGTGGCTGT-3′.

In situ hybridization by RNAscope

RNAscope® (Advanced Cell Diagnostics) was carried out on fixed and paraffin-embedded tissues according to the manufacturer's instructions. Target retrieval was achieved by heating the slides at 100 °C for 18 min. RNAscope® probes (Mm-Gdf2, Mm-Bmp10, negative Control Probe, and positive Control Probe) were incubated for 2 h at 40 °C on individual slides followed by hybridization amplification and staining. Sections were counterstained for 2 min with hematoxylin.

Author contributions—E. T., J.-J. F., and S. B. conceptualization; E. T., M. O., and A. D.-C. formal analysis; E. T., J.-J. F., and S. B. supervision; E. T., M. O., A. D.-C., C. M., M. S., R. D., A. L., and G. B. investigation; E. T., M. O., and A. D.-C. methodology; E. T. writing-original draft; E. T. project administration; E. T., J.-J. F., and S. B. writing-review and editing; S. B. funding acquisition.

Acknowledgments—We thank Dr. D. Constam (Ecole Polytechnique Fédérale de Lausanne, Switzerland) for his gift of PCR3-furin plasmid, Dr. S. J. lee (Johns Hopkins University School of Medicine, Baltimore, MD) and Dr. T. Zimmers (Thomas Jefferson University, Philadelphia, PA) for providing Bmp9-KO mice, Dr. D. Metzger (IGBMC, Illkirch, France) for providing the Rosa26-CreER^{T2} mouse, and the animal facility staff at Institut de Biosciences et Biotechnologies de Grenoble (BIG, Grenoble, France) for animal husbandry. We thank the Fondation Maladies Rares (FMR) for its financial support to the generation of Bmp10$^{lox/lox}$ mice.

References

1. Zinski, J., Tajer, B., and Mullins, M. C. (2017) TGF-β family signaling in early vertebrate development. *Cold Spring Harbor Perspect. Biol.* **2017,** 1101/cshperspect.a033274 Medline
2. Hinck, A. P., Mueller, T. D., and Springer, T. A. (2016) Structural biology and evolution of the TGF-β family. *Cold Spring Harbor Perspect. Biol.* **8,** pii: a022103 Medline
3. Constam, D. B. (2014) Regulation of TGFβ and related signals by precursor processing. *Semin. Cell Dev. Biol.* **32,** 85–97 Medline
4. Mueller, T. D., and Nickel, J. (2012) Promiscuity and specificity in BMP receptor activation. *FEBS Lett.* **586,** 1846–1859 CrossRef Medline
5. Miyazono, K., Kamiya, Y., and Morikawa, M. (2010) Bone morphogenetic protein receptors and signal transduction. *J. Biochem.* **147,** 35–51 CrossRef Medline
6. Garcia de Vinuesa, A., Abdelilah-Seyfried, S., Knaus, P., Zwijsen, A., and Bailly, S. (2016) BMP signaling in vascular biology and dysfunction. *Cytokine Growth Factor Rev.* **27,** 65–79 Medline
7. David, L., Mallet, C., Mazerbourg, S., Feige, J. J., and Bailly, S. (2007) Identification of BMP9 and BMP10 as functional activators of the orphan activin receptor-like kinase 1 (ALK1) in endothelial cells. *Blood* **109,** 1953–1961 CrossRef Medline
8. Scharpfenecker, M., van Dinther, M., Liu, Z., van Bezooijen, R. L., Zhao, Q., Pukac, L., Löwik, C. W., and ten Dijke, P. (2007) BMP-9 signals via ALK1 and inhibits bFGF-induced endothelial cell proliferation and VEGF-stimulated angiogenesis. *J. Cell Sci.* **120,** 964–972 CrossRef Medline
9. Johnson, D. W., Berg, J. N., Baldwin, M. A., Gallione, C. J., Marondel, I., Yoon, S. J., Stenzel, T. T., Speer, M., Pericak-Vance, M. A., Diamond, A., Guttmacher, A. E., Jackson, C. E., Attisano, L., Kucherlapati, R., Porteous, M. E., and Marchuk, D. A. (1996) Mutations in the activin receptor-like kinase 1 gene in hereditary haemorrhagic telangiectasia type 2. *Nat. Genet.* **13,** 189–195 CrossRef Medline
10. Oh, S. P., Seki, T., Goss, K. A., Imamura, T., Yi, Y., Donahoe, P. K., Li, L., Miyazono, K., ten Dijke, P., Kim, S., and Li, E. (2000) Activin receptor-like kinase 1 modulates transforming growth factor-β 1 signaling in the regulation of angiogenesis. *Proc. Natl. Acad. Sci. U.S.A.* **97,** 2626–2631 CrossRef Medline
11. Urness, L. D., Sorensen, L. K., and Li, D. Y. (2000) Arteriovenous malformations in mice lacking activin receptor-like kinase-1. *Nat. Genet.* **26,** 328–331 CrossRef Medline
12. Bidart, M., Ricard, N., Levet, S., Samson, M., Mallet, C., David, L., Subileau, M., Tillet, E., Feige, J. J., and Bailly, S. (2012) BMP9 is produced by hepatocytes and circulates mainly in an active mature form complexed to its prodomain. *Cell. Mol. Life Sci.* **69,** 313–324 CrossRef Medline
13. Neuhaus, H., Rosen, V., and Thies, R. S. (1999) Heart specific expression of mouse BMP-10 a novel member of the TGF-β superfamily. *Mech. Dev.* **80,** 181–184 CrossRef Medline
14. Chen, H., Shi, S., Acosta, L., Li, W., Lu, J., Bao, S., Chen, Z., Yang, Z., Schneider, M. D., Chien, K. R., Conway, S. J., Yoder, M. C., Haneline, L. S., Franco, D., and Shou, W. (2004) BMP10 is essential for maintaining cardiac growth during murine cardiogenesis. *Development* **131,** 2219–2231 CrossRef Medline
15. Chen, H., Brady Ridgway, J., Sai, T., Lai, J., Warming, S., Chen, H., Roose-Girma, M., Zhang, G., Shou, W., and Yan, M. (2013) Context-dependent

signaling defines roles of BMP9 and BMP10 in embryonic and postnatal development. *Proc. Natl. Acad. Sci. U.S.A.* **110,** 11887–11892 CrossRef Medline

16. Laux, D. W., Young, S., Donovan, J. P., Mansfield, C. J., Upton, P. D., and Roman, B. L. (2013) Circulating Bmp10 acts through endothelial Alk1 to mediate flow-dependent arterial quiescence. *Development* **140,** 3403–3412 CrossRef Medline
17. Levet, S., Ciais, D., Merdzhanova, G., Mallet, C., Zimmers, T. A., Lee, S. J., Navarro, F. P., Texier, I., Feige, J. J., Bailly, S., and Vittet, D. (2013) Bone morphogenetic protein 9 (BMP9) controls lymphatic vessel maturation and valve formation. *Blood* **122,** 598–607 CrossRef Medline
18. Levet, S., Ouarné, M., Ciais, D., Coutton, C., Subileau, M., Mallet, C., Ricard, N., Bidart, M., Debillon, T., Faravelli, F., Rooryck, C., Feige, J. J., Tillet, E., and Bailly, S. (2015) BMP9 and BMP10 are necessary for proper closure of the ductus arteriosus. *Proc. Natl. Acad. Sci. U.S.A.* **112,** E3207–E3215 CrossRef Medline
19. Ricard, N., Ciais, D., Levet, S., Subileau, M., Mallet, C., Zimmers, T. A., Lee, S. J., Bidart, M., Feige, J. J., and Bailly, S. (2012) BMP9 and BMP10 are critical for postnatal retinal vascular remodeling. *Blood* **119,** 6162–6171 CrossRef Medline
20. Brown, M. A., Zhao, Q., Baker, K. A., Naik, C., Chen, C., Pukac, L., Singh, M., Tsareva, T., Parice, Y., Mahoney, A., Roschke, V., Sanyal, I., and Choe, S. (2005) Crystal structure of BMP-9 and functional interactions with pro-region and receptors. *J. Biol. Chem.* **280,** 25111–25118 CrossRef Medline
21. Mi, L. Z., Brown, C. T., Gao, Y., Tian, Y., Le, V. Q., Walz, T., and Springer, T. A. (2015) Structure of bone morphogenetic protein 9 procomplex. *Proc. Natl. Acad. Sci. U.S.A.* **112,** 3710–3715 Medline
22. Sengle, G., Ono, R. N., Sasaki, T., and Sakai, L. Y. (2011) Prodomains of transforming growth factor β (TGFβ) superfamily members specify different functions: extracellular matrix interactions and growth factor bioavailability. *J. Biol. Chem.* **286,** 5087–5099 CrossRef Medline
23. Shi, M., Zhu, J., Wang, R., Chen, X., Mi, L., Walz, T., and Springer, T. A. (2011) Latent TGF-β structure and activation. *Nature* **474,** 343–349 CrossRef Medline
24. Wolfman, N. M., McPherron, A. C., Pappano, W. N., Davies, M. V., Song, K., Tomkinson, K. N., Wright, J. F., Zhao, L., Sebald, S. M., Greenspan, D. S., and Lee, S. J. (2003) Activation of latent myostatin by the BMP-1/tolloid family of metalloproteinases. *Proc. Natl. Acad. Sci. U.S.A.* **100,** 15842–15846 CrossRef Medline
25. Jiang, H., Salmon, R. M., Upton, P. D., Wei, Z., Lawera, A., Davenport, A. P., Morrell, N. W., and Li, W. (2016) The prodomain-bound form of bone morphogenetic protein 10 is biologically active on endothelial cells. *J. Biol. Chem.* **291,** 2954–2966 CrossRef Medline
26. Guo, J., and Wu, G. (2012) The signaling and functions of heterodimeric bone morphogenetic proteins. *Cytokine Growth Factor Rev.* **23,** 61–67 Medline
27. Hernandez, F., Huether, R., Carter, L., Johnston, T., Thompson, J., Gossage, J. R., Chao, E., and Elliott, A. M. (2015) Mutations in RASA1 and GDF2 identified in patients with clinical features of hereditary hemorrhagic telangiectasia. *Hum. Genome Var.* **2,** 15040 CrossRef Medline
28. Imayoshi, I., Ohtsuka, T., Metzger, D., Chambon, P., and Kageyama, R. (2006) Temporal regulation of Cre recombinase activity in neural stem cells. *Genesis* **44,** 233–238 CrossRef Medline
29. Kienast, Y., Jucknischke, U., Scheiblich, S., Thier, M., de Wouters, M., Haas, A., Lehmann, C., Brand, V., Bernicke, D., Honold, K., and Lorenz, S. (2016) Rapid activation of bone morphogenic protein 9 by receptor-mediated displacement of pro-domains. *J. Biol. Chem.* **291,** 3395–3410 CrossRef Medline
30. Zhao, B., Dong, X. S. X., Lu, C., and Springer, T. A. (2018) Prodomain: growth factor swapping in the structure of pro-TGF-β1. *J. Biol. Chem.* **295,** 1579–1589 Medline
31. O'Connor, M. B., Umulis, D., Othmer, H. G., and Blair, S. S. (2006) Shaping BMP morphogen gradients in the *Drosophila* embryo and pupal wing. *Development* **133,** 183–193 Medline
32. Shimmi, O., Umulis, D., Othmer, H., and O'Connor, M. B. (2005) Facilitated transport of a Dpp/Scw heterodimer by Sog/Tsg leads to robust patterning of the *Drosophila* blastoderm embryo. *Cell* **120,** 873–886 CrossRef Medline
33. Little, S. C., and Mullins, M. C. (2009) Bone morphogenetic protein heterodimers assemble heteromeric type I receptor complexes to pattern the dorsoventral axis. *Nat. Cell Biol.* **11,** 637–643 CrossRef Medline
34. Suzuki, A., Kaneko, E., Maeda, J., and Ueno, N. (1997) Mesoderm induction by BMP-4 and −7 heterodimers. *Biochem. Biophys. Res. Commun.* **232,** 153–156 CrossRef Medline
35. Butler, S. J., and Dodd, J. (2003) A role for BMP heterodimers in roof plate-mediated repulsion of commissural axons. *Neuron* **38,** 389–401 CrossRef Medline
36. Fuerer, C., Nostro, M. C., and Constam, D. B. (2014) Nodal.Gdf1 heterodimers with bound prodomains enable serum-independent nodal signaling and endoderm differentiation. *J. Biol. Chem.* **289,** 17854–17871 CrossRef Medline
37. Tanaka, C., Sakuma, R., Nakamura, T., Hamada, H., and Saijoh, Y. (2007) Long-range action of Nodal requires interaction with GDF1. *Genes Dev.* **21,** 3272–3282 CrossRef Medline
38. Mottershead, D. G., Sugimura, S., Al-Musawi, S. L., Li, J. J., Richani, D., White, M. A., Martin, G. A., Trotta, A. P., Ritter, L. J., Shi, J., Mueller, T. D., Harrison, C. A., and Gilchrist, R. B. (2015) Cumulin, an oocyte-secreted heterodimer of the transforming growth factor-β family, is a potent activator of granulosa cells and improves oocyte quality. *J. Biol. Chem.* **290,** 24007–24020 CrossRef Medline
39. Peng, J., Li, Q., Wigglesworth, K., Rangarajan, A., Kattamuri, C., Peterson, R. T., Eppig, J. J., Thompson, T. B., and Matzuk, M. M. (2013) Growth differentiation factor 9:bone morphogenetic protein 15 heterodimers are potent regulators of ovarian functions. *Proc. Natl. Acad. Sci. U.S.A.* **110,** E776–E785 CrossRef Medline
40. Ramirez, F., and Rifkin, D. B. (2009) Extracellular microfibrils: contextual platforms for TGFβ and BMP signaling. *Curr. Opin. Cell Biol.* **21,** 616–622 CrossRef Medline
41. Wohl, A. P., Troilo, H., Collins, R. F., Baldock, C., and Sengle, G. (2016) Extracellular regulation of bone morphogenetic protein activity by the microfibril component fibrillin-1. *J. Biol. Chem.* **291,** 12732–12746 CrossRef Medline
42. Sengle, G., Charbonneau, N. L., Ono, R. N., Sasaki, T., Alvarez, J., Keene, D. R., Bächinger, H. P., and Sakai, L. Y. (2008) Targeting of bone morphogenetic protein growth factor complexes to fibrillin. *J. Biol. Chem.* **283,** 13874–13888 CrossRef Medline
43. Aono, A., Hazama, M., Notoya, K., Taketomi, S., Yamasaki, H., Tsukuda, R., Sasaki, S., and Fujisawa, Y. (1995) Potent ectopic bone-inducing activity of bone morphogenetic protein-4/7 heterodimer. *Biochem. Biophys. Res. Commun.* **210,** 670–677 CrossRef Medline
44. Isaacs, M. J., Kawakami, Y., Allendorph, G. P., Yoon, B. H., Izpisua Belmonte, J. C., and Choe, S. (2010) Bone morphogenetic protein-2 and -6 heterodimer illustrates the nature of ligand-receptor assembly. *Mol. Endocrinol.* **24,** 1469–1477 CrossRef Medline
45. Israel, D. I., Nove, J., Kerns, K. M., Kaufman, R. J., Rosen, V., Cox, K. A., and Wozney, J. M. (1996) Heterodimeric bone morphogenetic proteins show enhanced activity *in vitro* and *in vivo*. *Growth Factors* **13,** 291–300 CrossRef Medline
46. Valera, E., Isaacs, M. J., Kawakami, Y., Izpisúa Belmonte, J. C., and Choe, S. (2010) BMP-2/6 heterodimer is more effective than BMP-2 or BMP-6 homodimers as inductor of differentiation of human embryonic stem cells. *PloS One* **5,** e11167 CrossRef Medline
47. Sebald, W., Nickel, J., Zhang, J. L., and Mueller, T. D. (2004) Molecular recognition in bone morphogenetic protein (BMP)/receptor interaction. *Biol. Chem.* **385,** 697–710 Medline
48. Allendorph, G. P., Isaacs, M. J., Kawakami, Y., Izpisua Belmonte, J. C., and Choe, S. (2007) BMP-3 and BMP-6 structures illuminate the nature of binding specificity with receptors. *Biochemistry* **46,** 12238–12247 CrossRef Medline
49. Mahlawat, P., Ilangovan, U., Biswas, T., Sun, L. Z., and Hinck, A. P. (2012) Structure of the Alk1 extracellular domain and characterization of its bone morphogenetic protein (BMP) binding properties. *Biochemistry* **51,** 6328–6341 CrossRef

50. Townson, S. A., Martinez-Hackert, E., Greppi, C., Lowden, P., Sako, D., Liu, J., Ucran, J. A., Liharska, K., Underwood, K. W., Seehra, J., Kumar, R., and Grinberg, A. V. (2012) Specificity and structure of a high affinity activin receptor-like kinase 1 (ALK1) signaling complex. *J. Biol. Chem.* **287,** 27313–27325 CrossRef Medline
51. Herrera, B., van Dinther, M., Ten Dijke, P., and Inman, G. J. (2009) Autocrine bone morphogenetic protein-9 signals through activin receptor-like kinase-2/Smad1/Smad4 to promote ovarian cancer cell proliferation. *Cancer Res.* **69,** 9254–9262 CrossRef Medline
52. Luo, J., Tang, M., Huang, J., He, B. C., Gao, J. L., Chen, L., Zuo, G. W., Zhang, W., Luo, Q., Shi, Q., Zhang, B. Q., Bi, Y., Luo, X., Jiang, W., *et al.* (2010) TGFβ/BMP type I receptors ALK1 and ALK2 are essential for BMP9-induced osteogenic signaling in mesenchymal stem cells. *J. Biol. Chem.* **285,** 29588–29598 CrossRef Medline
53. Mazerbourg, S., Sangkuhl, K., Luo, C. W., Sudo, S., Klein, C., and Hsueh, A. J. (2005) Identification of receptors and signaling pathways for orphan bone morphogenetic protein/growth differentiation factor ligands based on genomic analyses. *J. Biol. Chem.* **280,** 32122–32132 CrossRef Medline
54. Shimmi, O., Ralston, A., Blair, S. S., and O'Connor, M. B. (2005) The crossveinless gene encodes a new member of the Twisted gastrulation family of BMP-binding proteins which, with short gastrulation, promotes BMP signaling in the crossveins of the *Drosophila* wing. *Dev. Biol.* **282,** 70–83 CrossRef Medline
55. Miller, A. F., Harvey, S. A., Thies, R. S., and Olson, M. S. (2000) Bone morphogenetic protein-9: an autocrine/paracrine cytokine in the liver. *J. Biol. Chem.* **275,** 17937–17945 CrossRef Medline
56. Breitkopf-Heinlein, K., Meyer, C., König, C., Gaitantzi, H., Addante, A., Thomas, M., Wiercinska, E., Cai, C., Li, Q., Wan, F., Hellerbrand, C., Valous, N. A., Hahnel, M., Ehlting, C., Bode, J. G., *et al.* (2017) BMP-9 interferes with liver regeneration and promotes liver fibrosis. *Gut* **66,** 939–954 CrossRef Medline
57. David, L., Mallet, C., Keramidas, M., Lamandé, N., Gasc, J. M., Dupuis-Girod, S., Plauchu, H., Feige, J. J., and Bailly, S. (2008) Bone morphogenetic protein-9 is a circulating vascular quiescence factor. *Circ. Res.* **102,** 914–922 CrossRef Medline